LAWRENCE
LIVERMORE
NATIONAL
LABORATORY

LLNL-BOOK-836780

Chapter 8 - Small alcohols as biofuels: Status and needs for experimental data, theoretical calculations, and chemical kinetic modeling

C. Saggese, T. Chatterjee, W. J. Pitz

June 28, 2022

Combustion Chemistry and the Carbon Neutral Future: What will the next 25 years of research require?

Disclaimer

Small Alcohols as Low Carbon Fuels

Chiara Saggese and Tanusree Chatterjee, William J. Pitz*

Lawrence Livermore National Laboratory, Livermore, CA 94551, USA

KEYWORDS: Small alcohols, chemical kinetic model, low carbon fuels

*Corresponding Author:

William J. Pitz

Phone: 925-202-6918

Email: pitz1@llnl.gov

Submitted for a chapter in a book entitled "Combustion Chemistry and the Carbon Neutral Future: What will the next 25 years of research require"

April 1, 2022

Abstract

Small alcohols can be obtained from biomass and potentially meet economic and environmental goals for low carbon fuels. They can possibly meet fuel requirements of internal combustion engines and gas turbine engines used in the transportation sector during the transition period from fossil fuels to a carbon neutral future. To simulate the fuel effects of small alcohols in engine combustion, detailed chemical kinetic models of small alcohols are developed and reduced for use in multidimensional CFD codes to predict performance and emissions of advanced combustion engine designs. In this chapter, the status of detailed kinetic model mechanism development and research needs in the areas of theoretical understanding of their chemical kinetics, scope of experimental data and availability of chemical kinetic models are discussed for small alcohol fuels from C1 to C5. Future needs for accurate rate constants and deficiencies in current chemical kinetic models are identified as focus areas for future research.

1. Introduction

Achieving a carbon neutral future is a goal of 131 countries who have announced zero net carbon goals [1]. To achieve carbon neutrality, greenhouse gas emissions must be reduced and a large fraction of the greenhouse gas emissions in the world is from the transportation sector. For example in the United States, 27% of the global warming gases produced in 2020 were from the transportation sector [2]. As the world works towards its carbon neutrality goals, biofuels will likely be needed for the transportation sector in the transition period to reach carbon neutrality. Among the candidates for biofuels, small alcohols are of much interest because of their low cost and other favorable properties. Dunn et al. [3] evaluated 24 bio-derived fuels in the categories of the technological readiness, economic viability, and environmental benefits. When biochemical processing is used to produce these fuels, iso-butanol is an attractive fuel in all categories and cellulosic ethanol is similarly attractive, except for an unfavorable carbon efficiency which is in the environmental benefit category. When thermochemical processing is employed to produce the biofuels, methanol is attractive in all categories when syngas is used, and 1-butanol is unfavorable due to its co-production of valuable products (economic category) and its low carbon efficiency. Small alcohols are attractive for use in internal combustion (IC) engines. Alcohols with 1 - 4 carbon atoms have fuel properties that allow high thermodynamic efficiency for boosted spark-

ignition engines [4]. The thermodynamic efficiency of an IC engine is most sensitive to the maximum compression ratio that can be achieved in the engine. These small alcohols have high research octane number (RON) and high octane-sensitivity that allow operation of the engine with a higher compression ratio than current market fuels, achieving higher thermodynamic efficiency [4]. Another attractive property of small alcohols is that they are liquids that have a much higher energy density for use in transportation than gaseous, carbon-neutral fuels like hydrogen. Methanol, the smallest alcohol, has attracted attention for its use in marine vessels. Methanol made from woody biomass using gasification has low lifecycle emissions (wheels to hull) (6 g CO_2 equivalent / MJ-Fuel) compared to 96 for heavy fuel oil [5]. Methanol can be also be produced as an e-fuel with over 70% greenhouse gas reduction [6].

Longer chain alcohols, such as the propanol and butanol isomers, have benefits compared to ethanol, including higher energy density, lower water absorption, better miscibility with conventional fuels, and lower corrosivity [7]. It is notable that they have isometric structures, which is the primary difference in comparison with methanol and ethanol. Propanol is the smallest alcohol with two isomers, including n-propanol and iso-propanol. Butanol has four isomers, namely n-butanol, 2-butanol, iso-butanol, and tert-butanol. Among them, propanol isomers and iso-butanol have been identified by the U.S. Department of Energy's Co-Optimization of Fuels and Engines (Co-Optima) initiative [8] as attractive for commercialization as gasoline blending components. Iso-propanol can be produced through a gas fermentation process that utilizes waste gases (CO_2 and CO) [9]. As potential fuels for new advanced engines and for low-temperature combustion (LTC) applications, it is worth studying the autoignition chemistry of these alcohols.

Alcohols with up to five or even more carbon atoms are advantageous for practical use due to their high energy densities and low vapor pressure. Pentanol can be used as a neat fuel or fuel blending component in diesel [10] or jet engines [11]. Gaspar et al. [12] identified a fusel alcohol blend that contains two branched pentanols (2-methyl- and 3-methyl- 1-butanol) as a bio-derived fuel with the fewest barriers to market for spark-ignition, boosted engines.

These new biofuels need to be assessed for their suitability in current and future IC engine designs. Multidimensional, computational fluid dynamics (CFD) codes with reduced chemical kinetic models are used in the design process to achieve optimal engine designs for better performance, high-efficiency and low emissions. Once developed, detailed chemical kinetic models need to be reduced in size for use in these CFD codes.

In this chapter, the future needs for chemical kinetic models for biofuels are assessed going forward towards carbon neutrality by 2050. The needs for kinetic models include development of the reaction paths for these fuels, the accompanying pressure-dependent reaction rate constants, the thermodynamic properties, and the validation with experimental data.

In the chapter, we will first review each small alcohol for availability of detailed chemical kinetic models and experimental data needed for model validation. Also, needs for reaction path identification, rate constants and thermodynamic properties of species will be assessed. Finally, we will discuss the research needs for these alcohols as the world approaches its goal of carbon neutrality.

2. Small alcohol fuels

In this section, we review the literature for chemical kinetic models for each small alcohol fuel. We will assess the availability of experimental data for model validation and discuss the needs for future work, including needs for fundamental chemistry information and for experimental validation data.

2.1 Methanol

Methanol was one of the first kinetic mechanisms developed by Westbrook and Dryer (1979) [13] which was later improved by Held and Dryer (1998) [14]. Kovács et al. 2021 [15] recently reviewed the performance of 17 kinetic models for methanol that include its interaction with NO_x and found that the models from Glarborg et al. [16] and Shrestha et al. [17] performed best when their predictions are compared to a large set of experimental targets of ignition delay times (IDT) in shock tubes and species measurements in jet stirred reactors (JSR) and tubular-flow reactors.
To achieve improved kinetic model performance, it is important to identify the rate constants that have the largest influence on model predictions and determine more accurate estimates, if needed. In the case of methanol, Kovacs et al. [15] found that the most important reactions for the interaction between C_1 species and NOx are $CH_3OH + NO_2 = HONO + CH_2OH$ and $CH_2O + NO_2 = HONO + HCO$. Tao et al. [18] looked at the most impactful reactions which control methanol predictions of ignition delay times (IDTs) at 50 bar with simulated exhaust gas recirculation (EGR). The EGR was represented as a mixture of CO_2, H_2O, and N_2. They found the top reactions to be $CH_3OH + OH = CH_3O + H_2O$ for extinction in a perfectly stirred reactor (PSR) over the

temperature range of 300 to 900K and $CH_3OH + HO_2 = CH_2OH + H_2O_2$ for ignition in a PSR over the temperature range of 1000 to 1400K. This confirmed the findings of Klippenstein et al. [19] who found the $CH_3OH + HO_2$ reaction to be the most important reaction controlling the uncertainty of the IDTs of methanol at 20 bar and 1100 K. Klippenstein et al. also found that the $CH_3OH + O_2 = CH_2OH + HO_2$ reaction dominates the uncertainty in IDT at high pressure. They computed theoretical rate constants on both these reactions to improve the accuracy of the methanol kinetic model.

Recently, an updated methanol mechanism was published as part of the Combustion Chemistry Consortium (C3) project and its performance is documented in the supplementary material where predictions are compared to many experimental datasets [20]. This mechanism included a recently updated C1 base chemistry. An example of the current mechanism performance is seen in Fig. 1. In this case, the predictions are within the error bars experiments for about two thirds of the experimental points with the model underpredicting IDTs at 10 atm and at temperatures above 950 K by about 25%. [Insert Figure 1 here]

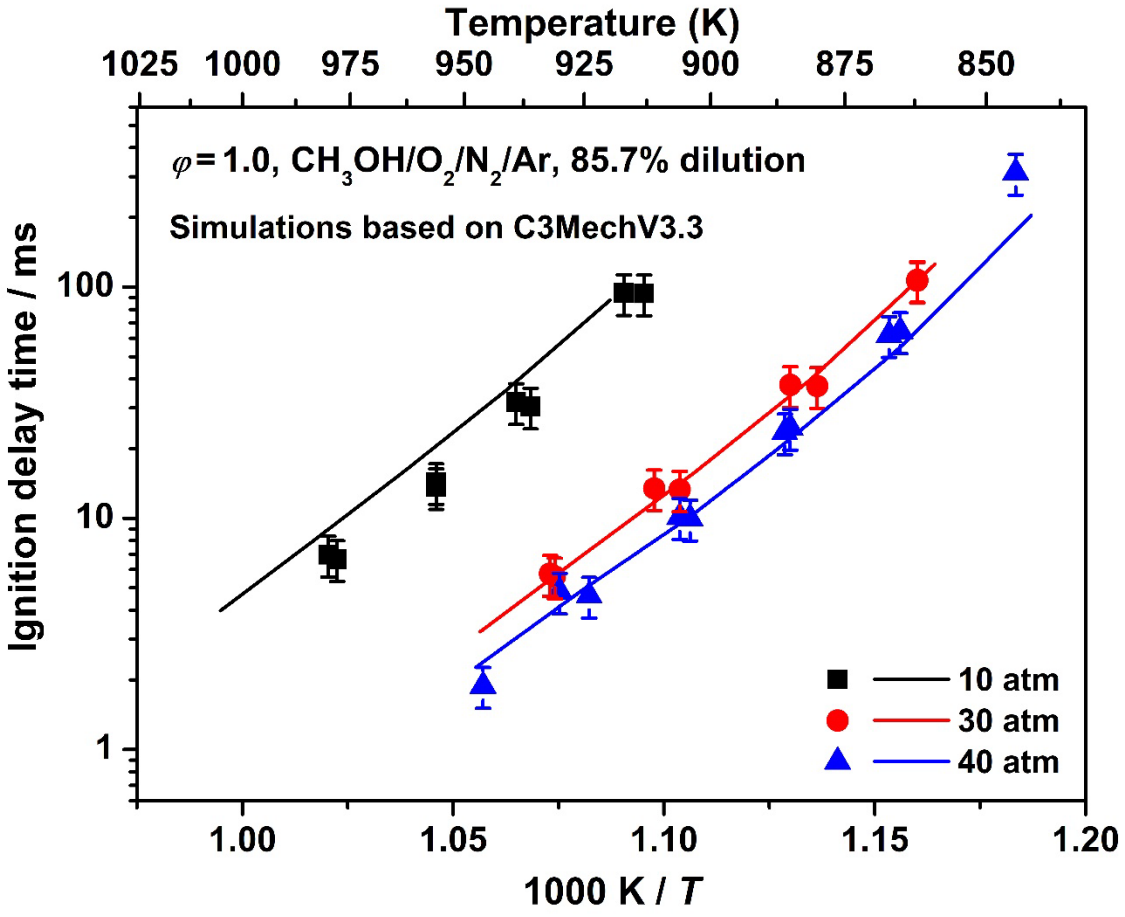

Figure 1: Behavior of C3 Mech kinetic model [20] at 10, 30 and 40 atm for stoichiometric mixtures of methanol in the rapid compression machine (RCM) [21].

For detailed mechanisms to be useful in the design of practical combustion devices, they need to be reduced in size so that they can be used in multidimensional simulation codes for the design of devices like internal combustion engines and gas turbine engines. Therefore, it is important to examine the available reduced models for methanol. Klippenstein et al. [19] have a reduced kinetic model for methanol of 21 species, but it does not include NOx chemistry. It was optimized and reduced from the Li et al. 2007 [22] mechanism and included new theoretically-based rate constants to improve the performance of the mechanism. A 40-species mechanism for methanol with NOx chemistry that was reduced from 151 species is available from Dong et al. [23]. This mechanism could be reduced further by using additional reduction techniques such as species lumping [24].

2.2 Ethanol

Ethanol is one of the major components of gasoline in the United States, whose concentration in market gasolines ranges from 10% (called E10) to 85% (called E85) by volume. The Co-Optimization of Fuels and Engines initiative (Co-Optima) of the U.S Department of Energy [8] investigated several candidates of biofuels and blends for internal combustion engines and ethanol was one of the blendstocks selected for advanced spark-ignition (SI) engines [8, 25].

Ethanol combustion has been studied extensively by researchers experimentally and numerically, as reviewed by Zyada and Samimi-Abianeh [26] and Roy and Askari [27]. Ethanol autoignition has been characterized in shock tubes (ST) at intermediate to high temperatures [28-31], and in rapid compression machines (RCMs) at low to intermediate temperatures [32-34] spanning a wide range of temperatures and pressures. Recently, Cheng et al. [35] investigated ethanol autoignition in a twin-piston rapid compression machine
at pressures of 20 and 40 bar, intermediate temperatures from 750 to 980 K, and two fuel loading conditions representative of boosted SI engines. Measured ignition delay times were compared to simulations using the mechanism developed by Saggese et al. [36] and good agreement was found, as shown in Fig. 2. [Insert Figure 2 here]

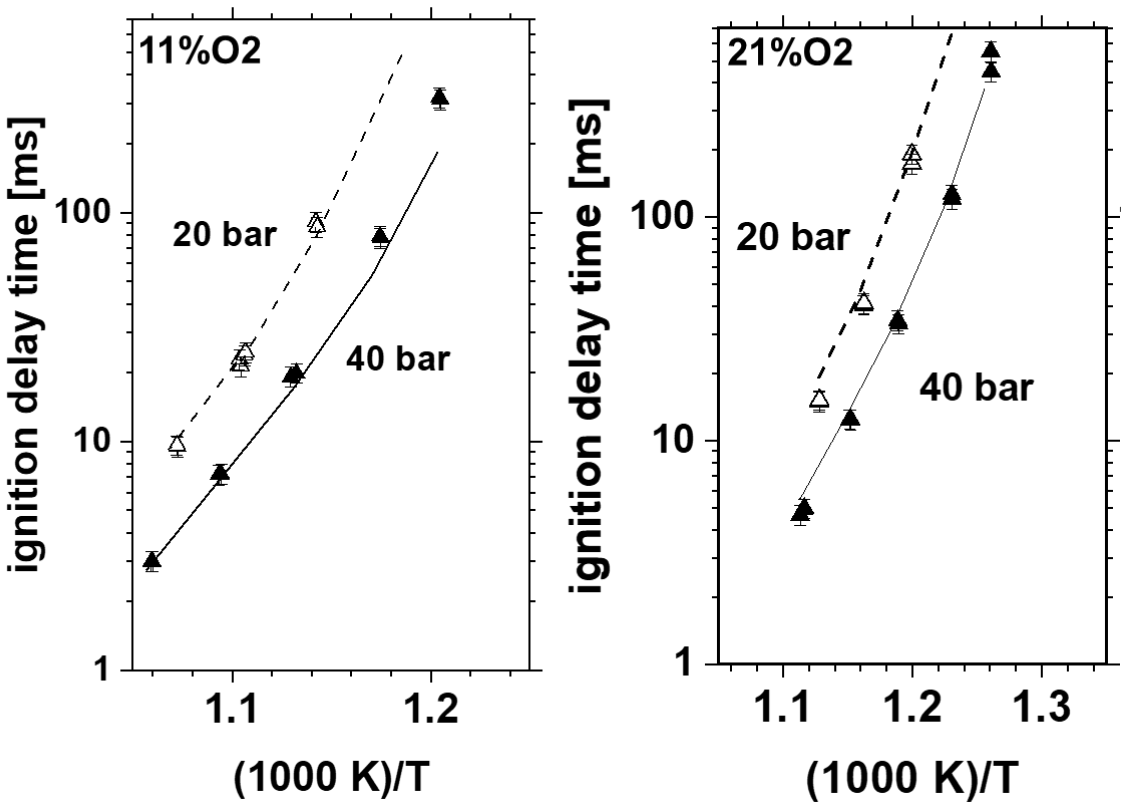

Figure 2. Measured and simulated ignition delay times for ethanol, presented as functions of inverse temperature; left panel: diluted condition and right panel: undiluted condition [35]. Symbols indicate experiments and lines indicate model results. Reprinted from Cheng et al. [35] with permission from Elsevier.

In Cheng et al. [35], sensitivity analysis to ignition delay time demonstrated the importance of H-abstraction reactions by OH and HO_2, and the branching ratio associated with these. Despite several studies on H-abstraction by OH from ethanol [37-39], discrepancies remain. Hashemi et al. [40] noted, that despite the consistency among the literature on the total rate coefficient for OH + ethanol → R + H_2O, branching fraction predictions are in substantial disagreement. The branching fractions are consistent in showing that α radicals (1-hydroxyethyl) are significantly favored. However, predictions of the formation of β radicals varies from < 5% to 20 – 25%. Hydrogen abstraction by HO_2 is significantly less facile than by OH and is dominated by reaction at the α site. Similar to OH, Hashemi et al. [40] noted discrepancies among chemical kinetics mechanisms for the abstraction reactions of ethanol with HO_2. An accurate determination of the

rate coefficients for these abstraction reactions is important to improve the reliability of modeling predictions.

Measurements of ethanol laminar burning velocity (LBV), which is a key metric to understand fuel performance and applicability in engines, have been carried out by different groups [41-44] Data from a laminar flow reactor at high-pressure [40], a jet stirred reactor and laminar flames [45] have been used to evaluate speciation of ethanol oxidation and pyrolysis. These fundamental experiments helped in developing and validating detailed kinetic models for ethanol oxidation under engine-relevant conditions.

Recently, ethanol combustion has been studied in blends with a full boiling range gasoline and gasoline surrogates to investigate autoignition and preliminary heat release characteristics at conditions representative of boosted spark-ignition and advanced compression-ignition engines [46, 47]. Cheng et al. [46, 47] performed experiments and kinetic modeling for the combustion of blends of ethanol and FACE (Fuels for Advanced Combustion Engines) gasoline F and its surrogates (FGF-LLNL and FGF-KAUST). They found that ethanol imposes only minor influences on intermediate temperature heat release (ITHR) and ignition reactivity for both surrogates within the intermediate temperature regime, but significantly suppresses low-temperature heat release (LTHR) and the low-temperature reactivity. The developed chemical model replicates the qualitative trends in autoignition and heat release characteristics, with better agreement at intermediate temperatures, while relatively greater discrepancies are observed at higher levels of ethanol blending, as seen in Fig. 3. This is primarily caused by the inadequately characterized interactions between the ethanol and surrogate sub-chemistries, highlighting the need to quantify the complex, non-fuel-specific intermolecular reactions between ethanol and each surrogate constitute. Moreover, differences in ethanol blending effects between the surrogates and FACE-F indicate the need to formulate more robust surrogates that better account for ethanol-blending effects. This could be achieved by including the properties of gasoline/ethanol blends, in addition to those of 'neat' gasolines, as targets to be matched. [Insert Figure 3 here]

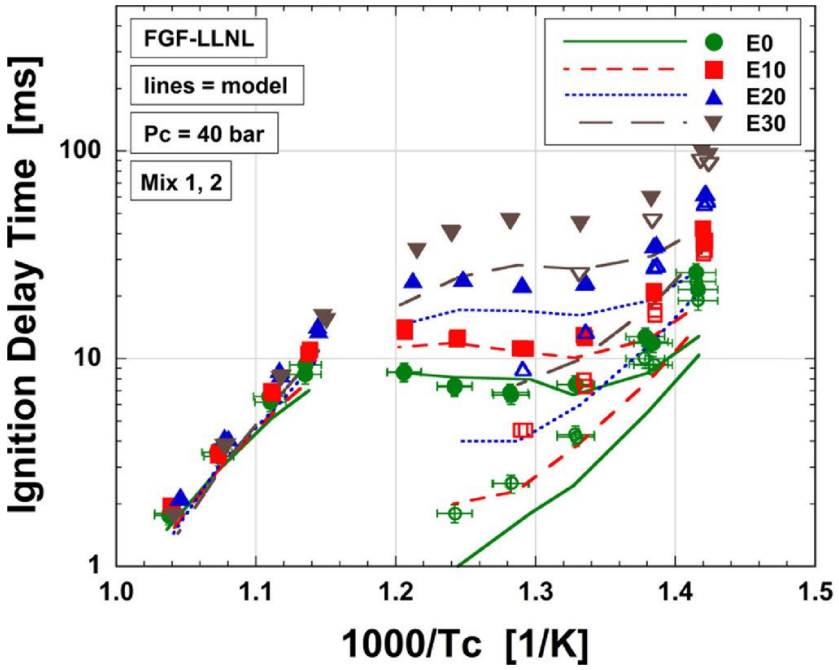

Figure 3. Experimental and modeled ignition delay times of gasoline surrogate FGF-LLNL with 0–30% vol./vol. ethanol blended at Pc = 40 bar, ϕ = 1, and 15% O_2. Symbols indicate experiment (open – first-stage; closes – main ignition) and lines are model results [47]. Reprinted from Cheng et al. [47] with permission from Elsevier.

Only few studies have been published on the interaction between NOx species (NO and NO_2) and ethanol. Ethanol oxidation in the presence of NO was studied by Alzueta and Hernández [48] in a flow reactor at atmospheric pressure and temperature range 700–1500 K from lean to rich conditions. Marrodán et al. [49] performed experiments of ethanol oxidation with and without NO in a flow reactor at high pressure (p = 20–60 bar) and a temperature range of 500–1100 K, spanning various equivalence ratios. They found that the presence of NO promotes ethanol oxidation, due to the increased relevance of the interactions of CH_3 radicals and NO_2 (from the conversion of NO to NO_2 at high pressures and in presence of O_2) and the increased concentration of OH radicals from the interaction of NO_2 and water. They used the kinetic model from Glarborg et al. [50] and modified it to better match their experimental data. However, their model could not capture the measured NO concentration profile at high pressure conditions. Recently, Shrestha et al. [17] well summarized the recent works on alcohol oxidation in the presence of NOx species. The authors also developed a kinetic model of methanol/NOx and ethanol/NOx oxidation, which was validated against a wide range of experiments.

2.3 Propanols

The combustion properties of propanol isomers were mainly studied in high-temperature conditions. Kasper et al. [51] studied the combustion chemistry of propanol isomers in flames by molecular-beam mass spectrometry. Johnson et al. [52] measured IDTs of propanol isomers in a shock tube between 1350 and 2000 K and found that n-propanol had higher reactivity than iso-propanol. According to their model, the reactivity of iso-propanol is limited by the dehydration reaction ($iC_3H_7OH \rightarrow C_3H_6+H_2O$), which produces propene and water and slows the chain branching. The kinetics of the dehydration reaction was studied by Heyne et al. [53] in a variable pressure flow reactor. The authors found that the measured dehydration rate constant was approximately a factor of four faster than the theoretical predictions of Bui et al. [54], thus they adjusted the pre-exponential factor of Bui et al. to produce a rate expression reconciled with their results. Togbe et al. [55] and Galmiche et al. [56] studied propanol isomers oxidation in a jet-stirred reactor (JSR) at 10 atm over the temperature range of 770–1190 K and equivalence ratios of 0.35–4.0. Flow reactor pyrolysis and laminar flame propagation were investigated for n-propanol and iso-propanol by Li et al. [57]. Ethylene and propene are respective dominant hydrocarbon products in the n-propanol and iso-propanol pyrolysis, while the most abundant oxygenated products are formaldehyde, acetaldehyde and ethenol in the n-propanol pyrolysis and acetone and acetaldehyde in the iso-propanol pyrolysis. Higher concentrations of aromatic and oxygenated pollutants were observed in the iso-propanol pyrolysis. A general trend that n-propanol has much faster laminar burning velocities (LBVs) than iso-propanol was noted under all investigated conditions.

Capriolo and Konnov [58] carried out LBV measurements with the heat flux method at T = 343–393 K, P = 1 atm and Φ=0.7–1.4, showing inconsistencies with the literature experiments performed using the spherical flame method. Beeckmann et al. [59] measured the laminar burning velocities (LBVs) of C1-C4 primary alcohols at a high pressure of 10 bar. Methanol burned faster than the other alcohols under fuel-rich conditions at both ambient and high pressures.

Recently, Cheng et al. [35] took measurements of IDTs of ethanol, the propanol isomers, 2- and iso-butanol under stoichiometric conditions between 750 and 980 K in a rapid compression

machine. The order of the reactivity of the five fuels changed, when the mixture changed from a diluted condition to a non-diluted condition. The absence of negative temperature coefficients (NTC) was observed for all the investigated alcohols under both non-diluted and diluted conditions. He et al. [60] extended the study of low-temperature combustion for propanol and butanol isomers in a rapid compression machine (RCM) under 90% dilution, at temperatures from 800 K to 1100 K, pressures of 20 and 40 bar and equivalence ratios of 0.25, 0.5 and 0.9. Under all investigated conditions, the order of reactivity among butanol isomers is consistent, namely n-butanol > iso-butanol ~= 2-butanol > tert–butanol, while n-propanol is always more reactive than iso-propanol. The reactivity of propanol isomers is similar to that of iso- and 2-butanol.

Recently, Saggese et al. [36] refined the kinetic model for C3-C4 linear and iso-alcohols from Sarathy et al. [61]. They updated the rate coefficients of H-atom abstraction reactions by OH and HO_2 from [33, 62], which play a major role in the ignition chemistry in the low-to-intermediate temperature range. This mechanism was proved to satisfactorily predict the IDTs of neat n-, iso-butanol and n-, iso-propanol in engine-relevant conditions.

The model by Saggese et al. [36] was tested against both sets of data at low-temperature and diluted conditions for propanol isomers, as shown in Fig. 4. The agreement is satisfactory across the whole range of temperatures, pressures and stoichiometries. [Insert Figure 4 here]

a)

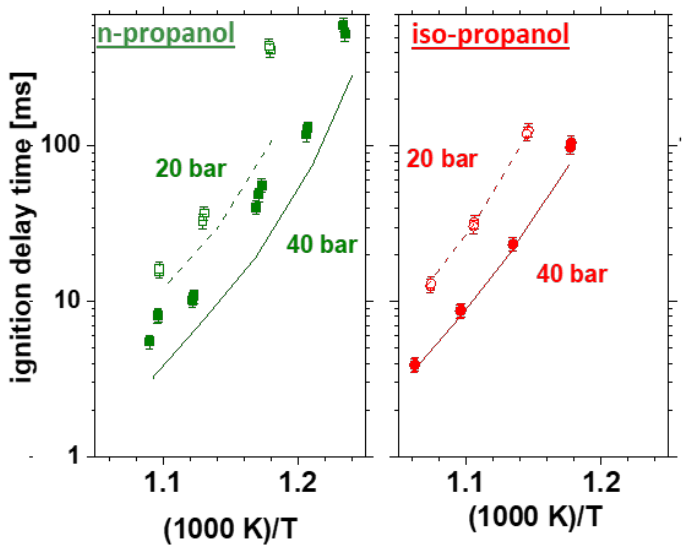

b)

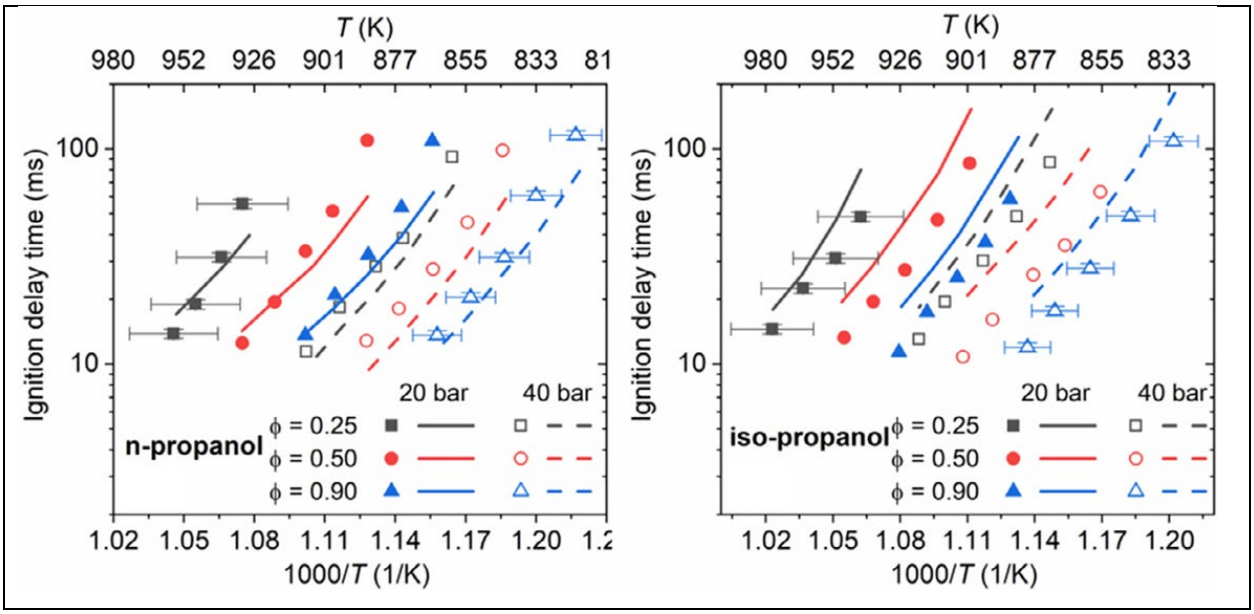

Figure 4. Measured and simulated ignition delay times for propanol isomers; panel a: diluted condition with 11% O_2 [35], and panel b: under 90% dilution [60]. Symbols indicate experiments and lines indicate model results. Reprinted from Cheng et al. [35] and He et al. [60] with permission from Elsevier.

Similarly to ethanol, the combustion of FACE F/iso-alcohol blends was also studied in a RCM at oxygenate blend levels of 0 to 30% vol/vol, at pressures of 20 and 40 bar, temperatures from 700 to 1000 K, and at dilute, stoichiometric fuel loading conditions (15% O_2, $\phi = 1$) [63]. At lower temperature conditions (700–860 K), the iso-alcohols are found to suppress first-stage reactivity and associated heat release with main ignition times extended. Reactivity suppression can be ranked as ethanol > iso-propanol > iso-butanol. At higher temperatures (860–1000 K) changes to fuel reactivity are less significant, where iso-propanol slightly suppresses reactivity, while iso-butanol promotes it. The detailed kinetic model developed by Saggese et al. [36] captures reasonably well the overall trends in the blending behavior and the effect of iso-propanol addition on IDTs, as shown in Fig. 5 for 20 and 40 bar. [Insert Figure 5 here]

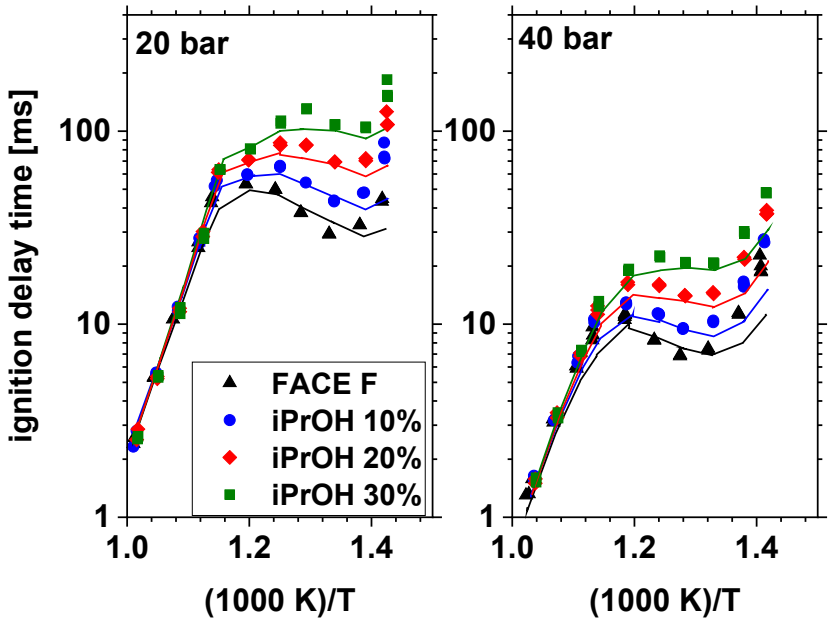

Figure 5. Experimental and modeled ignition delay times for FACE-F/iso-propanol blends at Pc = 20 bar and Pc = 40 bar, presented as functions of inverse temperature [63]. Mixtures are stoichiometric and dilute (15% O_2). Symbols indicate experiments, lines are model results.

Sensitivity analyses indicate that at Tc = 760 K, H-atom abstraction by OH from the gasoline surrogate fuel molecules (e.g., cyclopentane, iso-octane, n-heptane) are seen to be sensitive pathways controlling the main ignition time, while H-atom abstractions from iso-propanol and iso-butanol lead to alpha radicals, respectively, which act as scavengers in the system, and thus suppress reactivity. At the Tc = 900 K, similar chemistries are dominant, but there is an increasing importance of HO_2 as the H-atom abstractor.

2.4 Butanols

In comparison to propanol isomers, butanol isomers were studied more widely and prior studies have been well reviewed by Sarathy et al. [61]. For experimental work, both shock tube and RCM measurements of IDT's are available. For shock tube IDTs, they are available for neat n-butanol and other isomers [64-66] and neat iso-butanol [35, 67]. Moss et al. [64] studied the autoignition of four butanol isomers between 1200 and 1800 K in a shock tube and developed a detailed kinetic mechanism validated with their measurements. They found that the more reactive

n-butanol and iso-butanol were consumed mainly through H-abstraction, while the less reactive 2-butanol and tert–butanol were consumed primarily via dehydration. For RCM IDTs, experiments for all the neat butanols were carried out by Weber et al. [68] for air-like mixtures at ϕ = 0.5, 1 and 2. n-Butanol was found to be more reactive compared to the other three isomers. Also, experiments on all the isomers were recently published by He et al. [60] for 90% dilution over a range of stoichiometries from 0.25 to 0.9. Neither a NTC phenomenon nor a multi-stage ignition has been observed from their measurements. At a temperature range lower than 850 K, the reactivity of n-butanol was found to be much higher than the other fuels. In comparison, at temperatures higher than 900 K, the reactivity of tert–butanol was much lower than that of the other fuels. Additionally, n-butanol [69] and 2-butanol IDTs are available from [35]. For iso-butanol, RCM data experimental sets are available on IDTs [35] and on intermediate temperature heat release (ITHR) [70] .

Pelucchi et al. [71] measured IDTs of stoichiometric linear C3-C6 alcohols between 704 and 935 K in an RCM at 10 and 30 bar. There was no NTC behavior observed for ethanol, propanol and butanol. However, an apparent NTC behavior was found for n-pentanol.

JSR experimental speciation data on butanol isomers are also available from [72-75]. Dagaut et al. [76] found out that H-abstraction was the main pathway of n-butanol consumption in the JSR at 10 atm, while unimolecular decomposition was relatively negligible. Togbe et al. [73] carried out speciation measurements for 2- and iso-butanol at 10 atm in a JSR. They concluded that the oxidation rates of n-, 2-, and iso-butanol are similar but have different intermediate stable products. Lefkowitz et al. [74] observed large quantities of acetone and methane in the oxidation of tert–butanol at 780 K and 12.5 atm in the Princeton Variable Pressure Flow Reactor (VPFR). They observed that a lack of iso-butene production indicates that in these conditions tert-butanol is consumed by a bimolecular radical-oriented reaction rather than by molecular elimination to form water and iso-butene. Jin et al. [75] studied the combustion of tert-butanol experimentally in a flow reactor in pyrolysis conditions at 30–760 Torr, in a premixed laminar flat flame at 30 Torr and in a coflow methane/tert-butanol diffusion flame at atmospheric pressure. They found under pyrolysis and flame conditions, the unimolecular decomposition reaction is the dominant reaction among the fuel consumption pathways, in which four-center ring water elimination reaction has an extremely high contribution. iso-Butene and acetone were found to be the main primary products.

Various studies on laminar flame speeds on butanol isomers are present in literature [77-79]. Different groups found that the molecular structures of the butanol isomers have a significant influence on laminar flame speed (LFS). Gu et al. [77] investigated the LFS of butanol isomers and found that n-butanol/air mixtures had the highest LFS due to the highest number of inner C–H bonds, followed by 2-butanol, iso-butanol as well as tert-butanol, which was consistent with the results from Veloo et al. [78]. Wu and Law [79] concluded that the primary reason for the lowered flame speed of 2-butanol, iso-butanol and tert-butanol compared to n-butanol is that they crack into more branched intermediate species which are relatively stable, such as iso-butene, iso-propenol and acetone.

There have been many efforts to develop detailed kinetic models for butanol isomers [80-83] and these have been reviewed by Sarathy et al. [61] and He et al. [60]. One recent study on n-butanol and iso-butanol is from Saggese at al. [36]. As found in case of methanol, they found occasional difficulty in reconciling the simulation of multiple experimental data sets. As seen in Fig. 6, the simulated behavior for iso-butanol is slower compared to measured IDTs from one RCM [70] at 10 and 20 atm. However for another RCM [68], the simulations agree with experiments at 10 bar and are too fast at 30 bar. These differences occur even though experiments were at the same equivalence ratio and dilution. Numerical approaches are needed that can handle these discrepancies in the mechanism validation process. Other discrepancies were found by He et al. [60] who used the Sarathy et al. [80] kinetic model to simulate their RCM experiments for all four butanol isomers under dilute conditions over a wide range of stoichiometries. They found that the kinetic model did not sometimes reproduce the temperature dependence (i.e., activation energy) of the IDTs and this is another area for kinetic model improvements. In a fuel blending study, the IDTs of blends of iso-butanol with a research gasoline (FACE F) were examined in an RCM for dilute (15% O_2), stoichiometric mixtures [63]. When the kinetic model of Saggese at al. [36] was used to simulate the results, the simulated IDTs at the higher blend level (20-30%) were too fast compared to experiments (Fig. 7). Similar discrepancies were found in the case of methanol and ethanol. Further work is needed to improve the accuracy of kinetic models in simulating fuel-component interactions for these alcohol blends with gasoline. This may also warrant acquiring more experimental data on the interaction of butanol isomers with gasoline-type fuels. [Insert Figure 6 here] [Insert Figure 7 here]

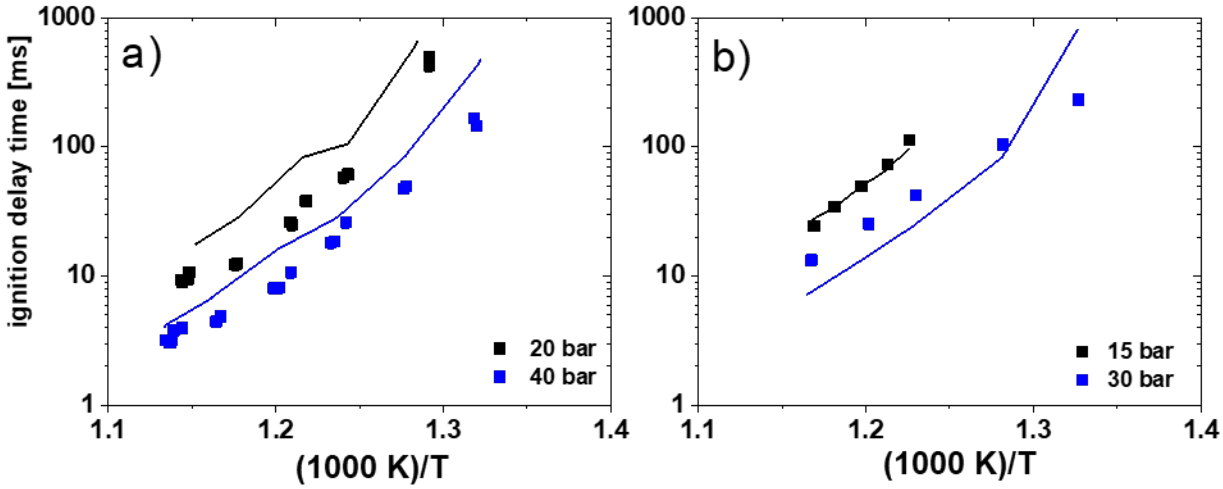

Figure 6. Measured (symbols) and simulated (solid lines) ignition delay times for: a) iso-butanol at φ = 1 with 21% O_2 in Ar and N_2 from an RCM [35]; b) iso-butanol at φ = 1 in air from an RCM [68]. Predictions are carried out using the model from Saggese et al. [36].

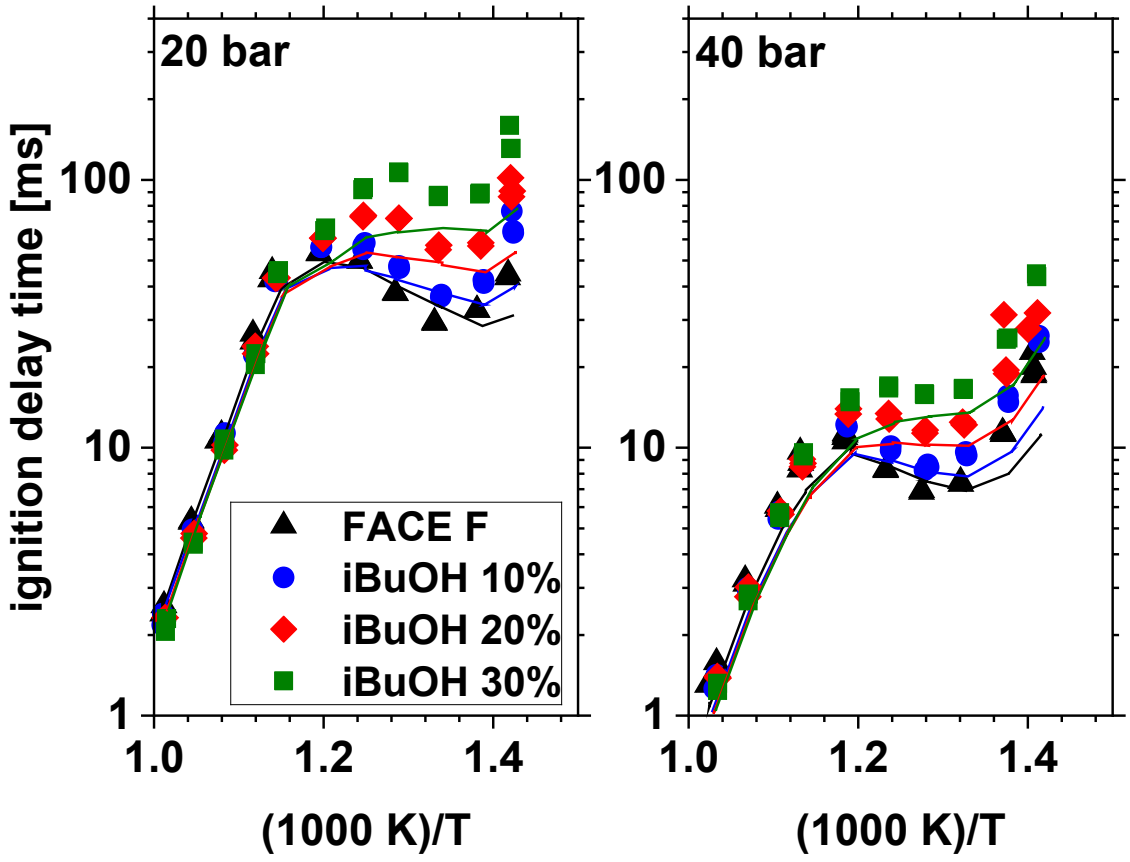

Figure 7. Experimental and modeled ignition delay times for FACE-F/iso-butanol blends at Pc = 20 bar and Pc = 40 bar, presented as functions of inverse temperature [63]. Mixtures are stoichiometric and dilute (15% O_2). Symbols indicate experiments, lines are model results.

Some recent efforts on fuel blending of butanols are the works of Michebalch et al. [84] for iso-butanol and Kalvakala et al. [85] for n-butanol. The blending of iso-butanol with a 5-component gasoline surrogate was carried out by Michelbach et al. [84] at conditions of 675–870 K, 20 bar, and Φ=1 within a RCM. The authors found that iso-butanol addition to gasoline produces interesting non-linear responses in terms of measured IDTs at low iso-butanol concentrations, similar to those previously observed for n-butanol blending [86]. Instead, Kalvakala et al. [85] performed computational fluid dynamics (CFD) simulations of a single-cylinder gasoline compression ignition (GCI) engine to investigate the impact of blending two biofuels, namely ethanol and n-butanol, with gasoline. The CFD model was employed to simulate the combustion of a gasoline-ethanol blend with 45% ethanol (E45) and a gasoline-butanol blend with 45% n-butanol (B45) under the same operating conditions to study the effects of fuel composition and start-of-injection (SOI) timing on combustion phasing and soot emissions. The sooting propensity followed the trend: B45>E20>E45 at all SOI conditions. Overall, it was observed that the autoignition phenomena was primarily related to fuel chemistry. On the other hand, the sooting propensity showed strong coupling with both fuel chemistry and physical properties, with greater impact of fuel physical properties at advanced SOI conditions.

2.5 Pentanols

Several chemical kinetic models of 1-pentanol oxidation have been developed based on analogies to smaller alcohols of similar structures using established reaction rate rules developed for alkanes and alcohols [61, 71]. The kinetic models have been validated using fundamental experiments on 1-pentanol combustion. The first kinetic model for 1-pentanol was proposed by Togbé et al. [87] for its high temperature (T>1000 K) oxidation. Heufer et al. [88] were the first to extend the 1-pentanol kinetic model to include both low- and high- temperature reaction classes. The authors observed that model predictions are highly sensitive to the rate constants in low temperature reaction classes such as $R+O_2$ (1^{st} O_2 addition) and $QOOH+O_2$ (2nd O_2 addition). To improve model predictions, Heufer et al. [88] altered the rate constant of reactions involving 1^{st}

and 2nd O_2 addition by a factor of 2–3, which lies within the uncertainty involved in the mechanism due to the lack of available theoretical calculations for reaction rates for low temperature reactions. Recently, Pelucchi et al. [89] developed an updated, comprehensive lumped kinetic model for n-C3−C6 alcohols pyrolysis and oxidation, and validated it against new ignition and speciation experiments.

To reduce uncertainty in the rate constants for reactions related to 1-pentanol, several theoretical studies using ab-initio methods have been undertaken. Zhao et al. [90] theoretically studied the unimolecular decomposition reactions of 1-pentanol at the CBS-QB3 level of theory. For H-atom abstraction reactions from 1-pentanol, Rawadieh et al. [91] recently calculated the rate expression for abstraction from the α-site by $H\dot{O}_2$, based on the CBS-QB3 method with transition state theory. For the 1-pentanol radical consumption, Van de Vijver et al. [92] explored their decomposition and isomerization reactions on potential energy surfaces (PESs) at the UCCSD(T)-F12a/cc-pVTZ-F12//M06-2X/6-311++G(d,p) level of theory and calculated the pressure-temperature dependence of the rate constants by solving the master equation. For low temperature reactions for 1-pentanol, a theoretical investigation has been conducted by Bu et al. [93] by employing the G4 compound method. They calculated the pressure-dependent rate constants for the reaction classes of R + O_2 = RO_2, RO_2 = QOOH, RO_2 = olefin + HO_2, and QOOH = cyclic ether + OH. Very recently, Duan et al. [94] performed ab-initio calculations at the CCSD(T)/aug-cc-pVTZ//M06-2X/cc-pVTZ level on the fate of the 1-hydroxy-1-peroxypentyl radical. Duan et al. [94] and others [93, 95, 96] identified HO_2 elimination from α-alcohol peroxy radical forming aldehyde and HO_2 as the most important alcohol-specific reaction that competes with the low-temperature chain-branching channels and inhibits the fuel reactivity at low temperatures. The incorporation of these theoretically derived rate constants into the 1-pentanol chemical mechanisms has been shown to improve the model performance [92, 94]. Recently, based on ab-initio calculations, Lockwood et al. [97] calculated the rate constants for important low temperature reaction classes such as R+O_2=RO_2 and RO_2=QOOH at the CCSD(T)/cc-pV∞Z level of theory. Using newly calculated pressure-temperature dependent rate constants for 1-pentanol, a new kinetic model for low temperature oxidation of 1-pentanol has been developed by Chatterjee et al. [98]. Unlike previous models which were based on analogy to ethanol oxidation, the newly developed kinetic model for 1-pentanol by Chatterjee et al. [98] shows that at engine-relevant pressure conditions (≥30 bar), the major intermediate species 1-pentanal formed during 1-pentanol

oxidation primarily forms via a stabilized adduct pathway ($R+O_2<=>R\dot{O}_2<=>aldehyde+HO_2$), rather than the chemically activated pathway ($R+O_2<=>aldehyde+HO_2$). The newly proposed model is in good agreement with the experiments across a wide range of temperature and pressure. Figure 8 shows the comparison of Chatterjee et al.'s [98] kinetic model to experimental data for 1-pentanol obtained from using both the high-pressure shock tube (HPST) and RCM facilities at NUI Galway (NUIG) [98]. [Insert Figure 8 here]

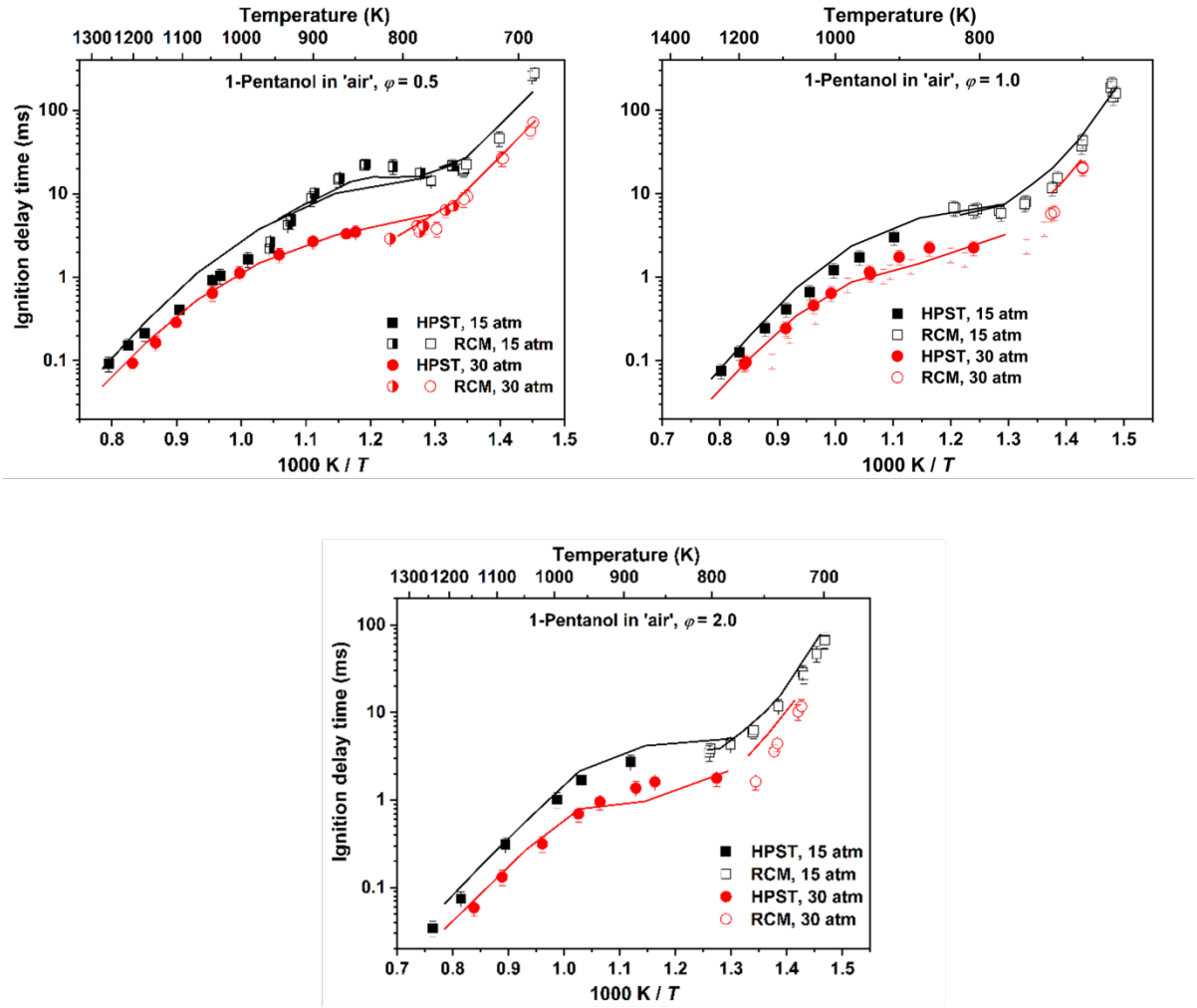

Figure 8. Comparison of simulated (solid lines) and measured (symbols) IDTs [98] for 1-pentanol at P=15 and 30 bar, φ=0.5, 1 & 2, 21% O_2 in N_2/Ar. The closed symbols are from the HPST, and the open and half-filled symbols from the RCM.

Regarding other straight-chain pentanol isomers, secondary C5 alcohols such as 2- and 3-pentanols have been identified as potential alternative fuels or blending components for modern engines. The first high-temperature kinetic model for all three straight-chain pentanol isomers was developed by Köhler et al. [99]. For 3-pentanol, Carbonnier et al. [100] developed a high-temperature kinetic model oxidation and validated it using speciation data from a jet-stirred reactor (JSR) and IDTs from a shock tube (ST). For theoretical studies, Feng et al. [101] recently calculated the rate constants for H-atom abstraction reactions from 3-pentanol by $\dot{H}$, $\dot{C}H_3$, $H\dot{O}_2$, and $\dot{O}H$ radicals and updated the Carbonnier et al. [100] model. Regarding 2-pentanol, Bai et al. [102] theoretically studied the radical decomposition kinetics in detail. Dayma et al. [103] used the newly calculated rate constants by Bai et al. [102] involving 2-pentanol radical decomposition kinetics to construct and validate a new high-temperature kinetic model using high-pressure JSR and ST experimental data. Recently, a low temperature kinetic model for 2- and 3-pentanol has been developed by Chatterjee et al. [98] for the first time. In these kinetic models, rate constants for important low temperature reaction classes initiated by $R+O_2$ reactions are based on theoretical calculations for 1-pentanol by Lockwood et al. [97]. The proposed kinetic model for 2- and 3-pentanol by Chatterjee et al. [98] including both high temperature and low temperature reaction classes have been validated against HPST & RCM data obtained using experimental facilities at NUI Galway (NUIG) [98] as well as experimental data available in the literature [100-103]. Figure 9 shows the comparison of simulations using the Chatterjee et al. kinetic model [98] to IDT experimental data for 2- and 3-pentanol in a HPST and RCM [98]. [Insert Figure 9 here].

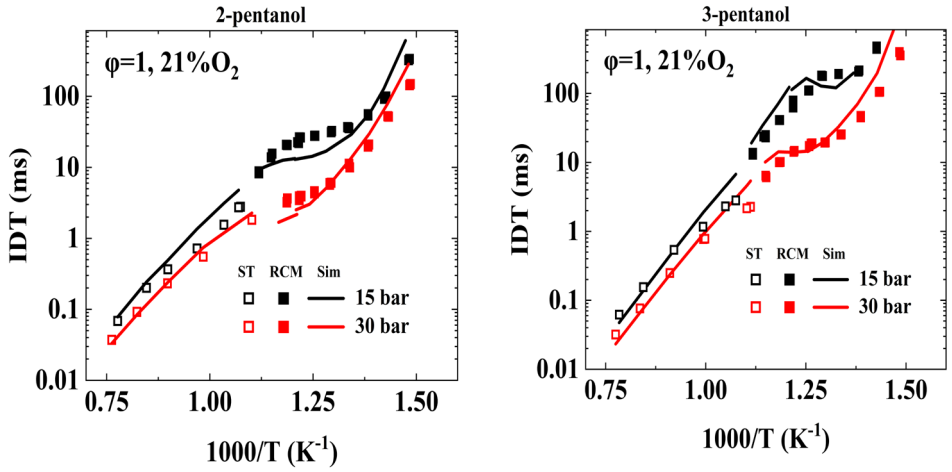

Figure 9. Comparison of NUIG's experimental data (symbols) and simulations predicted IDTs (solid lines) for 2- and 3- pentanol at P=15 and 30 bar, φ=1, 21% O_2 in N_2/Ar. The open symbols are for the Shock Tube (ST) and the closed symbols are for the RCM [98]. Simulations use the Chatterjee et al. kinetic model [98].

For branched pentanols, Tsujimura et al. [104, 105] developed a detailed chemical kinetic model for iso-pentanol (3-methyl-butan-1-ol) and used it to simulate homogeneous-charge compression-ignition (HCCI) combustion. Dayma et al. [106] measured species concentrations in a JSR (jet stirred reactor) over a range of equivalence ratios and temperatures at 10 atm and proposed a detailed chemical kinetic model of iso-pentanol. A detailed reaction mechanism of iso-pentanol including a wide range of temperature, pressure and equivalence ratio was developed by Sarathy et al. [61], and validated against previous and new experimental data. Their results show that iso-pentanol is less reactive than1-pentanol. Recently, Cao et al. [107] revisited the pyrolysis of iso-pentanol with flow reactor experiments at 30 and 760 torr and they developed a pyrolysis kinetic model. Comparing their results with similar data of 1-pentanol and 2-methylbutan-1-ol pyrolysis, they found that the initial decomposition temperatures of the two branched pentanol isomers are slightly lower than that of 1-pentanol at both pressures and that the concentrations of benzene and fulvene in the pyrolysis of the two branched pentanol isomers are significantly higher than those in the pyrolysis of n-pentanol.

Tang et al. [108] measured the high temperature ignition behavior of C5 alcohols (1-pentanol, iso-pentanol, and 2-methylbutan-1-ol) in the temperature ranging from 1100 to 1500 K and

pressures of 1.0 and 2.6 atm. A high temperature chemical kinetic model for 2-methylbutan-1-ol was proposed and compared against their ignition data. Serinyel et al. [109] measured the species concentrations at 10 atm, from lean to rich conditions in a jet-stirred reactor (JSR) and simulated their measurements using a detailed chemical kinetic mechanism. Later, Zhang et al. [110] measured pyrolysis products of 2-methylbutan-1-ol in a flow reactor at low and atmospheric pressures and tested a kinetic model against their measurements. The results indicate that the decomposition of 2-methylbutanol is similar to iso-butanol rather than n-butanol.

Park [111] et al. were the first to study the low-temperature chemistry of 2-methylbutan-1-ol with a high-pressure shock tube experiments at temperatures from 750 to 1250 K and pressures at 20 and 40 bar and with detailed kinetic modeling. The ignition delay times of 2-methylbutan-1-ol/air mixtures at intermediate temperatures are similar to those of iso-pentanol, while the reactivity of 2-methylbutan-1-ol is higher than iso-pentanol in the high temperature region. Up to now, no ignition experiments of 2-methylbutan-1-ol ignition were carried out at lower temperatures (e.g. ~650 K) using a rapid compression machine. However, new ignition delay time data of 2-methylbutan-1-ol combustion at lean and high-pressure conditions have recently been acquired and a new kinetic model has been developed, which will be included in a forthcoming paper that is currently under preparation.

Laminar flames speeds of these pentanol isomers were measured and compared first by Li et al. [112] and recently by Nativel [113] et al. who found 1-pentanol flame speeds being higher than those from Li et al. Laminar flame speeds of pentanol isomer-air mixtures were found to decrease in the order of 1-pentanol > 2-methylbutan-1-ol > iso-pentanol.

3. Recommendations for future work and future directions

3.1 Methanol

Given the large amount of experimental data on methanol (for example, see the supplementary data of Dong et al. [20]), it is difficult to identify conditions where further progress in accuracy can be made for methanol. This is also true for other alcohols that have large amounts of experimental data like ethanol. Some simulations show good agreement and others do not when compared to experiments at similar conditions of temperature, pressure, and equivalence ratio. Numerical tools are needed to identify specific regions of temperature, pressure, equivalence ratio

and dilution where discrepancies between predictions and experimental measurements exist so that these conditions can be studied in experiments and kinetically analyzed. Then the further progress in kinetic-model accuracy can be made. Also, because of advancements in the accuracy of theoretically-based rate constants and thermodynamic properties, it is important to use theoretically-based methods to increase the accuracy the rate constants and thermodynamic properties and potentially improve the accuracy of kinetic model predictions of methanol and other alcohols.

3.2 Ethanol

Despite several studies on H-abstraction by OH from ethanol [37-39], discrepancies remain. Hashemi et al. [40] noted that despite the consistency among the literature on the total rate coefficient for OH + ethanol → R + H_2O, branching fraction predictions are in substantial disagreement. Similar to OH, Hashemi et al. [40] also noted discrepancies among chemical kinetics mechanisms for abstraction reactions of ethanol with HO_2. A more accurate determination of the rate coefficients for these abstraction reactions is important to improve the reliability of modeling predictions.

There are needs for the understanding of ethanol oxidation in the presence of NO. When ethanol is oxidized with NO in a flow reactor at high-pressure, the kinetic model modified by Glarborg et al. [50] could not capture the measured NO concentration profile for high pressure conditions. Also, it should be noted that combined studies of methanol and ethanol fuel interaction with NOx have not been published so far, neither from an experimental nor from a modeling point of view. Therefore, more experimental work focusing on NOx/fuel interaction is required for arriving at an improved mechanistic understanding for methanol and ethanol, being the basis for future studies on NOx formation and fuel interaction during the combustion of larger alcohols.

In the rapid compression machine experiments, discrepancies were noted when ethanol was mixed with a research gasoline and its surrogates at higher levels of ethanol blending [46, 47]. This is primarily caused by the inadequately characterized interactions between the ethanol and surrogate sub-chemistries, highlighting the need to quantify the complex, non-fuel-specific intermolecular reactions between ethanol and each surrogate constitute. Moreover, differences in ethanol blending effects between the surrogates and FACE-F indicate the need to formulate more robust surrogates that better account for ethanol-blending effects. This could be achieved by

including experiments on gasoline/ethanol blends, in addition to those of 'neat' gasolines, as targets to be matched.

3.3 Propanol

The kinetics of propanol isomers is not studied as much as the other alcohols and requires more experimental and theoretical investigation. For iso-propanol, there are inconsistencies of a factor of four between the rate of its dehydration reaction ($iC_3H_7OH \rightarrow C_3H_6+H_2O$) from theoretical calculations and from fundamental experiments. For all alcohols, experimental measurements of rate coefficients for H-abstraction are absent in the 400 –900 K range [114].

No detailed theoretical studies on the reactions between propanol isomers and CH_3 at the molecular level have been reported in literature until two recent studies appeared. Nguyen et al. [115] investigated the mechanisms and kinetics of the reactions of methyl radical with n/i-propanol (n/i-C_3H_7OH) in detail using density functional theory and coupled cluster theory with rate constant prediction. Their analysis suggests that the H-cleavage from C–H bonding of C-atom bonded to –OH group plays a significant role in the H-abstraction reactions and, at the same conditions, the reaction of methyl radical with iso-propanol takes place faster than with n-propanol. Similarly, Shi and Song [116] studied H-abstraction reaction by H and CH_3 at the M06-2X level of theory. They found that for n-propanol the H-abstraction channels from the α-CH_2 group are kinetically more favorable. For the iso-propanol + R (R = H, CH_3•) reactions, the H-abstraction channels from the -CH group are predominant at low-temperature.

Moreover, the study on H-atom abstraction reactions from propanol isomers by HO_2 is very scarce. Rawadieh et al. [91] recently carried out a theoretical study on the H-atom abstraction reactions from C1–C5 alcohols by HO_2, but only the rate constants of the H-atom abstraction reactions from the weakest carbon sites were reported. A more comprehensive investigation was recently reported by Duan et al. [117] who calculated the rate constants of all the possible H-atom abstraction reaction channels from propanol isomers by HO_2 using the multistructural variational transition state theory (MS-VTST). These rate constants calculated for propanol isomers are lower than the recent calculations reported by Rawadieh et al. [91] by several orders of magnitude. This significant discrepancy highlights the importance of accurate theoretical efforts. Moreover, the rates from Duan et al. [117] for propanol isomers were directly tested in the model of Saggese et al. [36], showing suppression of fuel oxidation reactivity, leading to longer ignition delay times

and retarded fuel consumption, in particular at low temperatures and high pressures. The updated Saggese et al. model shows better predictions in the mole fractions of aldehydes, despite less satisfactory performance for iso-propanol oxidation.

In the Saggese et al. kinetic modeling study [36], the rate of abstraction by OH from propanol isomers was taken from the McGillen et al. [62] study on butanol isomers. While this was a successful approach for the Saggese et al. study, more theoretical or experimental studies on OH abstraction rates are needed for the pentanol isomers to verify this approach.

He et al. [60] studied both propanol isomers under dilute conditions over a range of lean stoichiometries in an RCM. They tested many kinetic models and found that the Saggese et al. [36] model most accurately simulated their experimental results. However, they found that the kinetic model was inconsistent in simulating the measured activation energies of IDTs on Arrhenius plots. They stated that further work on the propanol kinetic models is needed to resolve these discrepancies.

3.4 Butanol

As in case of methanol, occasional difficulty is found in reconciling the simulation of multiple experimental data sets for iso-butanol at similar experimental conditions [36]. Strategies are needed in mechanism validation workflows to deal with this issue. Also, in the case for methanol and ethanol, a recent butanol model showed difficulty in simulating iso-butanol blends at high levels in gasoline [70]. More experimental studies of butanol isomers blended with full-boiling gasoline fuels are needed to help resolve these difficulties. Additionally, although Sarathy et al. [80] kinetic model was identified as the best literature model for simulating the He et al. [60] butanol isomer IDTs at diluted/lean conditions, this model sometimes had difficulty in reproducing the experimental temperature dependence of the IDTs. Finally, theoretical calculations of R + O_2 for butanol isomer radicals and the successive low-temperature chemistry classes are still very few, with the newest effort being from Labbe et al. [97]. More such theoretical studies are needed. These issues remain for future work for butanol isomers.

3.5 C5 branched alcohols

Despite progress, further fundamental chemical kinetic studies are needed for larger alcohols. Specifically, a comprehensive theoretical study for various channels on R + O_2 potential energy

surfaces is needed to determine low temperature reaction rate rules for branched C5 fuels. A first attempt to calculate kinetic constants for 1-pentanol oxidation chemistry has been carried out in the work of Chatterjee et al. [98]. Such studies will improve the model's predictive capabilities at high-pressure and lean conditions, which are typical of new, advanced high-efficiency, low-emission engines.

4. Summary and Recommendations

Small alcohol fuels can be made from low carbon feedstocks through biochemical processes that meet technical requirements and economic goals. Methanol, ethanol, and isomers of propanol, butanol and pentanol have been found to be suitable for use in internal combustion engines and have been identified by the Co-Optima project as having low barriers for market adoption. Detailed chemical kinetic models are needed to assess the impact of small alcohol fuel properties on engine combustion. In this chapter, the state of development of chemical kinetic models for small alcohols is assessed and future needs for the advancement of such models are identified. Methanol and ethanol have been studied widely experimentally and many chemical kinetic models have been developed and reported in the literature. For methanol with its large set of experimental validation data, there are instances when experiments at similar conditions in the shock tube and/or RCM show agreement and disagreement with the kinetic model. Further work is needed to resolve these differences help identify the causes of agreement and disagreement. With ethanol, some disagreement is seen when blending at higher levels of ethanol in a research gasoline when computed IDTs are compared to the experimental data in the RCM. Also, significant discrepancies remain the literature about what abstraction rate by OH to use for ethanol. For iso-propanol, there are inconsistencies of a factor of four between the rate of its dehydration reaction (iC$_3$H$_7$OH→C$_3$H$_6$+H$_2$O) based on theoretical calculations and from fundamental experiments. For C5 alcohols, more theoretical calculations are needed on their low temperature reaction channels on the R + O$_2$ potential energy surface to potentially help increase the accuracy of the associated chemical kinetic models.

Acknowledgements

This work was performed under the auspices of the U.S. Department of Energy (DOE) by Lawrence Livermore National Laboratory under Contract DE-AC52-07NA27344 and was

conducted as part of the Co-Optimization of Fuels & Engines (Co-Optima) initiative sponsored by the DOE Office of Energy Efficiency and Renewable Energy (EERE), Bioenergy Technologies and Vehicle Technologies Offices. The authors thank Dr. Shijun Dong for producing Figure 1.

References

1. T. Hale, T. Kuramochi, J. Lang, B. Mapes, S. Smith, R. Aiyer, R. Black, M. Boot, P. Chalkley, F. Hans, N. Hay, A. Hsu, N. Höhne, S. Mooldijk, T. Walsh Net Zero Tracker. https://www.zerotracker.net/ (April 20, 2022)
2. EPA https://www.epa.gov/ghgemissions/sources-greenhouse-gas-emissions#t1fn2 (April 20, 2022)
3. J. B. Dunn, M. Biddy, S. Jones, H. Cai, P. T. Benavides, J. Markham, L. Tao, E. Tan, C. Kinchin, R. Davis, A. Dutta, M. Bearden, C. Clayton, S. Phillips, K. Rappé, P. Lamers, ACS Sustainable Chemistry & Engineering 6 (1) (2018) 561-569.
4. J. P. Szybist, S. Busch, R. L. McCormick, J. A. Pihl, D. A. Splitter, M. A. Ratcliff, C. P. Kolodziej, J. M. E. Storey, M. Moses-DeBusk, D. Vuilleumier, M. Sjöberg, C. S. Sluder, T. Rockstroh, P. Miles, Progress in Energy and Combustion Science 82 (2021) 100876.
5. A. Foretich, G. G. Zaimes, T. R. Hawkins, E. Newes, Maritime Transport Research 2 (2021) 100033.
6. J. Messner, T. Hawkins, L. Kindberg Current State of Sustainable Marine Fuels. https://www.energy.gov/eere/bioenergy/beto-webinars (March 15, 2022, Slide 47)
7. K. Kohse-Höinghaus, P. Oßwald, T. A. Cool, T. Kasper, N. Hansen, F. Qi, C. K. Westbrook, P. R. Westmoreland, Angewandte Chemie International Edition 49 (21) (2010) 3572-3597.
8. J. T. Farrell, J. Holladay, R. Wagner, *Co-Optimization of Fuels & Engines: Fuel Blendstocks with the Potential to Optimize Future Gasoline Engine Performance; Identification of Five Chemical Families for Detailed Evaluation*, NREL/TP-5400-69009; DOE/GO-102018-4970, 2018.
9. F. E. Liew, R. Nogle, T. Abdalla, B. J. Rasor, C. Canter, R. O. Jensen, L. Wang, J. Strutz, P. Chirania, S. De Tissera, A. P. Mueller, Z. Ruan, A. Gao, L. Tran, N. L. Engle, J. C. Bromley, J. Daniell, R. Conrado, T. J. Tschaplinski, R. J. Giannone, R. L. Hettich, A. S. Karim, S. D. Simpson, S. D. Brown, C. Leang, M. C. Jewett, M. Köpke, Nature Biotechnology 40 (3) (2022) 335-344.
10. N. Yilmaz, A. Atmanli, Fuel 210 (2017) 75-82.
11. L. Chen, S. Ding, H. Liu, Y. Lu, Y. Li, A. P. Roskilly, Applied Energy 203 (2017) 91-100.
12. D. J. Gaspar, B. H. West, D. Ruddy, T. J. Wilke, E. Polikarpov, T. L. Alleman, A. George, E. Monroe, R. W. Davis, D. Vardon, A. D. Sutton, C. M. Moore, P. T. Benavides, J. Dunn, M. J. Biddy, S. B. Jones, M. D. Kass, J. A. Pihl, J. A. Pihl, M. M. Debusk, M. Sjoberg, J. Szybist, C. S. Sluder, G. Fioroni, W. J. Pitz, *Top Ten Blendstocks Derived From Biomass For Turbocharged Spark Ignition Engines: Bio-blendstocks With Potential for Highest Engine Efficiency*, PNNL-28713 United States 10.2172/1567705 PNNL English, Pacific Northwest National Lab. (PNNL), Richland, WA (United States), 2019.
13. C. K. Westbrook, F. L. Dryer, Combust. Sci. Technol. 20 (3-4) (1979) 125-140.
14. T. J. Held, F. L. Dryer, Int. J. Chem. Kinet. 30 (11) (1998) 805-830.

15. M. Kovács, M. Papp, I. G. Zsély, T. Turányi, Int. J. Chem. Kinet. 53 (7) (2021) 884-900.
16. P. Glarborg, J. A. Miller, B. Ruscic, S. J. Klippenstein, Progress in Energy and Combustion Science 67 (2018) 31-68.
17. K. P. Shrestha, L. Seidel, T. Zeuch, F. Mauss, Combust. Sci. Technol. 191 (9) (2019) 1627-1659.
18. Y. Tao, G. P. Smith, H. Wang, Combust. Flame 195 (2018) 18-29.
19. S. J. Klippenstein, L. B. Harding, M. J. Davis, A. S. Tomlin, R. T. Skodje, Proc. Combust. Inst. 33 (1) (2011) 351-357.
20. S. Dong, S. W. Wagnon, L. Pratali Maffei, G. Kukkadapu, A. Nobili, Q. Mao, M. Pelucchi, L. Cai, K. Zhang, M. Raju, T. Chatterjee, W. J. Pitz, T. Faravelli, H. Pitsch, P. K. Senecal, H. J. Curran, Applications in Energy and Combustion Science 9 (2022) 100043.
21. U. Burke, W. K. Metcalfe, S. M. Burke, K. A. Heufer, P. Dagaut, H. J. Curran, Combust. Flame 165 (2016) 125-136.
22. J. Li, Z. Zhao, A. Kazakov, M. Chaos, F. L. Dryer, J. J. Scire Jr., Int. J. Chem. Kinet. 39 (3) (2007) 109-136.
23. Y. Dong, X. Wang, Z. Ma, X. Li, Y. Jin, International Journal of Energy Research 46 (6) (2022) 7861-7871.
24. H. Huang, M. Fairweather, J. F. Griffiths, A. S. Tomlin, R. B. Brad, Proc. Combust. Inst. 30 (1) (2005) 1309-1316.
25. R. L. McCormick, G. Fioroni, L. Fouts, E. Christensen, J. Yanowitz, E. Polikarpov, K. Albrecht, D. J. Gaspar, J. Gladden, A. George, SAE International Journal of Fuels and Lubricants 10 (2) (2017) 442-460.
26. A. Zyada, O. Samimi-Abianeh, Energy & Fuels 33 (8) (2019) 7791-7804.
27. S. Roy, O. Askari, Energy & Fuels 34 (3) (2020) 3691-3708.
28. M. P. Dunphy, J. M. Simmie, Journal of the Chemical Society, Faraday Transactions 87 (11) (1991) 1691-1696.
29. L. R. Cancino, M. Fikri, A. A. M. Oliveira, C. Schulz, Energy & Fuels 24 (5) (2010) 2830-2840.
30. K. A. Heufer, H. Olivier, Shock Waves 20 (4) (2010) 307-316.
31. K. Heufer, Y. Uygun, H. Olivier, S. Vranckx, C. Lee, R. Fernandes in: *Experimental study of the high-pressure ignition of alcohol based biofuels*, Proc. European Combust Meeting, 2011.
32. C. Lee, S. Vranckx, K. A. Heufer, S. V. Khomik, Y. Uygun, H. Olivier, R. X. Fernandez, Zeitschrift für Physikalische Chemie 226 (1) (2012) 1-28.
33. G. Mittal, S. M. Burke, V. A. Davies, B. Parajuli, W. K. Metcalfe, H. J. Curran, Combust. Flame 161 (5) (2014) 1164-1171.
34. C. L. Barraza-Botet, S. W. Wagnon, M. S. Wooldridge, The Journal of Physical Chemistry A 120 (38) (2016) 7408-7418.
35. S. Cheng, D. Kang, S. S. Goldsborough, C. Saggese, S. W. Wagnon, W. J. Pitz, Proc. Combust. Inst. 38 (1) (2021) 709-717.
36. C. Saggese, C. M. Thomas, S. W. Wagnon, G. Kukkadapu, S. Cheng, D. Kang, S. S. Goldsborough, W. J. Pitz, Proc. Combust. Inst. 38 (1) (2021) 415-423.
37. R. Sivaramakrishnan, M. C. Su, J. V. Michael, S. J. Klippenstein, L. B. Harding, B. Ruscic, The Journal of Physical Chemistry A 114 (35) (2010) 9425-9439.
38. S. Xu, M. C. Lin, Proc. Combust. Inst. 31 (1) (2007) 159-166.
39. J. Zheng, D. G. Truhlar, Faraday discussions 157 (2012) 59-88.
40. H. Hashemi, J. M. Christensen, P. Glarborg, Fuel 218 (2018) 247-257.
41. S. Y. Liao, D. M. Jiang, Z. H. Huang, K. Zeng, Q. Cheng, Applied Thermal Engineering 27 (2-3) (2007) 374-380.
42. J. Liang, G. Li, Z. Zhang, Z. Xiong, F. Dong, R. Yang, Energy & Fuels 28 (7) (2014) 4754-4761.
43. N. Hinton, R. Stone, R. Cracknell, C. Olm, Fuel 214 (2018) 127-134.
44. L. van Treek, M. Lubrano Lavadera, L. Seidel, F. Mauss, A. A. Konnov, Fuel 257 (2019) 116069.

45. N. Leplat, P. Dagaut, C. Togbé, J. Vandooren, Combust. Flame 158 (4) (2011) 705-725.
46. S. Cheng, D. Kang, A. Fridlyand, S. S. Goldsborough, C. Saggese, S. Wagnon, M. J. McNenly, M. Mehl, W. J. Pitz, D. Vuilleumier, Combust. Flame 216 (2020) 369-384.
47. S. Cheng, C. Saggese, D. Kang, S. S. Goldsborough, S. W. Wagnon, G. Kukkadapu, K. Zhang, M. Mehl, W. J. Pitz, Combust. Flame 228 (2021) 57-77.
48. M. U. Alzueta, J. M. Hernandez, Energy & Fuels 16 (1) (2002) 166-171.
49. L. Marrodán, Á. J. Arnal, Á. Millera, R. Bilbao, M. U. Alzueta, Fuel 223 (2018) 394-400.
50. P. Glarborg, M. U. Alzueta, K. Dam-Johansen, J. A. Miller, Combust. Flame 115 (1-2) (1998) 1-27.
51. T. Kasper, P. Osswald, U. Struckmeier, K. Kohse-Hoinghaus, C. A. Taatjes, J. Wang, T. A. Cool, M. E. Law, A. Morel, P. R. Westmoreland, Combust. Flame 156 (6) (2009) 1181-1201.
52. M. V. Johnson, S. S. Goldsborough, Z. Serinyel, P. O'Toole, E. Larkin, G. O'Malley, H. J. Curran, Energy & Fuels 23 (12) (2009) 5886-5898.
53. J. S. Heyne, S. Dooley, Z. Serinyel, F. L. Dryer, H. Curran, Zeitschrift für Physikalische Chemie 229 (6) (2015) 881-907.
54. B. H. Bui, R. S. Zhu, M. C. Lin, The Journal of Chemical Physics 117 (24) (2002) 11188-11195.
55. C. Togbé, P. Dagaut, F. Halter, F. Foucher, Energy & Fuels 25 (2) (2011) 676-683.
56. B. Galmiche, C. Togbé, P. Dagaut, F. Halter, F. Foucher, Energy & Fuels 25 (5) (2011) 2013-2021.
57. W. Li, Y. Zhang, B. Mei, Y. Li, C. Cao, J. Zou, J. Yang, Z. Cheng, Combust. Flame 207 (2019) 171-185.
58. G. Capriolo, A. A. Konnov, Combust. Flame 218 (2020) 189-204.
59. J. Beeckmann, L. Cai, H. Pitsch, Fuel 117, Part A (0) (2014) 340-350.
60. X. He, Q. Wang, R. Fernandes, B. Shu, Combust. Flame 237 (2022) 111818.
61. S. M. Sarathy, P. Oßwald, N. Hansen, K. Kohse-Höinghaus, Progress in Energy and Combustion Science 44 (2014) 40-102.
62. M. R. McGillen, M. Baasandorj, J. B. Burkholder, The Journal of Physical Chemistry A 117 (22) (2013) 4636-4656.
63. S. S. Goldsborough, S. Cheng, D. Kang, C. Saggese, S. W. Wagnon, W. J. Pitz, Proc. Combust. Inst. 38 (4) (2021) 5655-5664.
64. J. T. Moss, A. M. Berkowitz, M. A. Oehlschlaeger, J. Biet, V. Warth, P. A. Glaude, F. Battin-Leclerc, J. Phys. Chem. A 112 (43) (2008) 10843-10855.
65. K. A. Heufer, R. X. Fernandes, H. Olivier, J. Beeckmann, O. Röhl, N. Peters, Proc. Combust. Inst. 33 (1) (2011) 359-366.
66. I. Stranic, D. P. Chase, J. T. Harmon, S. Yang, D. F. Davidson, R. K. Hanson, Combust. Flame 159 (2) (2012) 516-527.
67. L. Pan, Y. Zhang, Z. Tian, F. Yang, Z. Huang, Energy & Fuels 28 (3) (2014) 2160-2169.
68. B. W. Weber, C.-J. Sung, Energy & Fuels 27 (3) (2013) 1688-1698.
69. B. W. Weber, K. Kumar, Y. Zhang, C.-J. Sung, Combust. Flame 158 (5) (2011) 809-819.
70. S. Cheng, S. S. Goldsborough, S. W. Wagnon, W. J. Pitz, Combust. Flame 233 (2021) 111602.
71. M. Pelucchi, S. Namysl, E. Ranzi, A. Rodriguez, C. Rizzo, K. P. Somers, Y. Zhang, O. Herbinet, H. J. Curran, F. Battin-Leclerc, T. Faravelli, Energy & Fuels (2020).
72. P. Dagaut, S. M. Sarathy, M. J. Thomson, Proc. Combust. Inst. In Press, Corrected Proof (2009).
73. C. Togbé, A. Mzé-Ahmed, P. Dagaut, Energy & fuels 24 (9) (2010) 5244-5256.
74. J. K. Lefkowitz, J. S. Heyne, S. H. Won, S. Dooley, H. H. Kim, F. M. Haas, S. Jahangirian, F. L. Dryer, Y. Ju, Combust. Flame 159 (3) (2012) 968-978.
75. H. Jin, J. Cai, G. Wang, Y. Wang, Y. Li, J. Yang, Z. Cheng, W. Yuan, F. Qi, Combust. Flame 169 (2016) 154-170.
76. P. Dagaut, S. M. Sarathy, M. J. Thomson, Proc. Combust. Inst. 32 (1) (2009) 229-237.
77. X. Gu, Z. Huang, S. Wu, Q. Li, Combust. Flame 157 (12) (2010) 2318-2325.

78. P. S. Veloo, F. N. Egolfopoulos, Proc. Combust. Inst. 33 (1) (2011) 987-993.
79. F. Wu, C. K. Law, Combust. Flame 16o (12) (2013) 2744-2756.
80. S. M. Sarathy, S. Vranckx, K. Yasunaga, M. Mehl, P. Oßwald, W. K. Metcalfe, C. K. Westbrook, W. J. Pitz, K. Kohse-Höinghaus, R. X. Fernandes, H. J. Curran, Combust. Flame 159 (6) (2012) 2028–2055.
81. R. Grana, A. Frassoldati, T. Faravelli, U. Niemann, E. Ranzi, R. Seiser, R. Cattolica, K. Seshadri, Combust. Flame 57 (11) (2010) 2137-2154.
82. S. S. Merchant, E. F. Zanoelo, R. L. Speth, M. R. Harper, K. M. Van Geem, W. H. Green, Combust. Flame 160 (2013) 1907-1929.
83. J. Cai, W. Yuan, L. Ye, Z. Cheng, Y. Wang, W. Dong, L. Zhang, Y. Li, F. Zhang, F. Qi, Combust. Flame 161 (8) (2014) 1955-1971.
84. C. Michelbach, A. Tomlin, Int. J. Chem. Kinet. 53 (6) (2021) 787-808.
85. K. C. Kalvakala, P. Pal, J. P. Gonzalez, C. P. Kolodziej, H. J. Seong, G. Kukkadapu, M. McNenly, S. Wagnon, R. Whitesides, N. Hansen, S. K. Aggarwal, Fuel 319 (2022) 123740.
86. I. Gorbatenko, A. S. Tomlin, M. Lawes, R. F. Cracknell, Proc. Combust. Inst. 37 (1) (2019) 501-509.
87. C. Togbé, F. Halter, F. Foucher, C. Mounaim-Rousselle, P. Dagaut, Proc. Combust. Inst. 33 (1) (2011) 367-374.
88. K. A. Heufer, S. M. Sarathy, H. J. Curran, A. C. Davis, C. K. Westbrook, W. J. Pitz, Energy & Fuels 26 (11) (2012) 6678-6685.
89. M. Pelucchi, S. Namysl, E. Ranzi, A. Rodriguez, C. Rizzo, K. P. Somers, Y. Zhang, O. Herbinet, H. J. Curran, F. Battin-Leclerc, T. Faravelli, Energy & Fuels 34 (11) (2020) 14708-14725.
90. L. Zhao, L. Ye, F. Zhang, L. Zhang, The Journal of Physical Chemistry A 116 (37) (2012) 9238-9244.
91. S. E. Rawadieh, I. S. Altarawneh, M. A. Batiha, L. A. Al-Makhadmeh, M. H. Almatarneh, M. Altarawneh, Energy & Fuels 33 (11) (2019) 11781-11794.
92. R. Van de Vijver, K. M. Van Geem, G. B. Marin, J. Zádor, Combust. Flame 196 (2018) 500-514.
93. L. Bu, P. N. Ciesielski, D. J. Robichaud, S. Kim, R. L. McCormick, T. D. Foust, M. R. Nimlos, The Journal of Physical Chemistry A 121 (29) (2017) 5475-5486.
94. Y. Duan, M. Monge-Palacios, E. Grajales-Gonzalez, D. Han, K. H. Møller, H. G. Kjaergaard, S. M. Sarathy, Combust. Flame 219 (2020) 20-32.
95. J. Zador, R. X. Fernandes, Y. Georgievskii, G. Meloni, C. A. Taatjes, J. A. Miller, Proc. Combust. Inst. 32 (2009) 271-277.
96. O. Welz, J. Zador, J. D. Savee, L. Sheps, D. L. Osborn, C. A. Taatjes, J. Phys. Chem. A 117 (46) (2013) 11983-12001.
97. K. S. Lockwood, S. C. Stutzman, N. A. Huq, S. F. Ahmed, T. D. Foust, N. J. Labbe, Green Chemistry (2022) submitted.
98. T. Chatterjee, C. Saggese, S. Dong, V. Patel, K. S. Lockwood, H. J. Curran, N. J. Labbe, S. W. Wagnon, W. J. Pitz, Proc. Combust. Inst. (2022) submitted.
99. M. Köhler, T. Kathrotia, P. Oßwald, M. L. Fischer-Tammer, K. Moshammer, U. Riedel, Combust. Flame 162 (9) (2015) 3197-3209.
100. M. Carbonnier, Z. Serinyel, A. Kéromnès, G. Dayma, B. Lefort, L. Le Moyne, P. Dagaut, Proc. Combust. Inst. 37 (1) (2019) 477-484.
101. Y. Feng, J. Zhu, S. Wang, L. Yu, Z. He, Y. Qian, X. Lu, The Journal of Physical Chemistry A (2021).
102. J. Bai, Y. Zhu, C.-W. Zhou, G. Dayma, Z. Serinyel, P. Dagaut, Proc. Combust. Inst. 38 (1) (2021) 823-832.
103. G. Dayma, Z. Serinyel, M. Carbonnier, J. Bai, Y. Zhu, C.-W. Zhou, A. Kéromnès, B. Lefort, L. Le Moyne, P. Dagaut, Proc. Combust. Inst. 38 (1) (2021) 833-841.
104. T. Tsujimura, W. J. Pitz, Y. Yang, J. E. Dec, SAE Int. J. Fuels Lubr. 4 (2) (2011) 257-270.
105. T. Tsujimura, W. J. Pitz, F. Gillespie, H. J. Curran, B. W. Weber, Y. Zhang, C.-J. Sung, Energy & Fuels 26 (8) (2012) 4871-4886.

106. G. Dayma, C. Togbe, P. Dagaut, Energy & Fuels 25 (11) (2011) 4986–4998.
107. C. Cao, Y. Zhang, X. Zhang, J. Zou, F. Qi, Y. Li, J. Yang, Fuel 257 (2019) 116039.
108. C. Tang, L. Wei, X. Man, J. Zhang, Z. Huang, C. K. Law, Combust. Flame 160 (3) (2013) 520-529.
109. Z. Serinyel, C. Togbé, G. Dayma, P. Dagaut, Combust. Flame 161 (12) (2014) 3003-3013.
110. X. Zhang, B. Yang, W. Yuan, Z. Cheng, L. Zhang, Y. Li, F. Qi, Proc. Combust. Inst. 35 (1) (2015) 409-417.
111. S. Park, O. Mannaa, F. Khaled, R. Bougacha, M. S. Mansour, A. Farooq, S. H. Chung, S. M. Sarathy, Combust. Flame 162 (5) (2015) 2166-2176.
112. Q. Li, C. Tang, Y. Cheng, L. Guan, Z. Huang, Energy & Fuels 29 (8) (2015) 5334-5348.
113. D. Nativel, M. Pelucchi, A. Frassoldati, A. Comandini, A. Cuoci, E. Ranzi, N. Chaumeix, T. Faravelli, Combust. Flame 166 (2016) 1-18.
114. B. Rotavera, C. A. Taatjes, Progress in Energy and Combustion Science 86 (2021) 100925.
115. T. Huu Nguyen, T. Nghia Nguyen, G. Huong Thi Vu, H. Minh Thi Nguyen, Computational and Theoretical Chemistry 1210 (2022) 113638.
116. G. Shi, J. Song, Computational and Theoretical Chemistry 1211 (2022) 113688.
117. Y. Duan, Z. Huang, D. Han, Combust. Flame 231 (2021) 111495.